2021 European Control Conference (ECC)
June 29 - July 2, 2021. Rotterdam, Netherlands

# Attitude observers for three-vehicle heterogeneous formations based on the Lagrange-d'Alembert principle

Pedro Cruz[1], Pedro Batista[2], and Amit Sanyal[3]

*Abstract*— **This paper considers the problem of attitude estimation in three-vehicle heterogeneous formations with no line of sight between two of the vehicles. Each vehicle measures different inertial reference vectors and directions to other vehicles. The relative direction between the two vehicles with no line of sight cannot be measured. Moreover, rate gyros measure the angular velocity of each vehicle. An attitude observer is designed based on the Lagrange-d'Alembert principle of variational mechanics, considering only kinematic models. This design is driven by the angular velocity measurement and a reconstructed attitude computed from the direction measurements. The attitude reconstruction follows a deterministic algorithm, which has a unique solution under appropriate assumptions. The attitude observer is locally exponentially stable and the estimation error is shown to converge to zero for almost all initial conditions. The discrete-time form of the observer is obtained for practical implementation. Lastly, numerical simulations validate the stability and convergence characteristics of the observer.**

## I. Introduction

Attitude gives the relation between different coordinate frames, often between a body-fixed frame and an inertial frame. It usually provides critical information for guidance, navigation, control, and other systems.

Attitude estimation methods try to find the best value for the attitude that fits a series of measurements taken over time. Early methods include deterministic approaches such as the Tri-Axial Attitude Determination (TRIAD) algorithm [1] and solutions of the Wahba's problem [2], of which [3] and [4] are just examples. Estimation schemes accounting for prior estimates have also been developed early in the field, many based on the extended Kalman filter (EKF) [5]. Methods seeking stability and convergence properties include nonlinear observers [6], cascade observers [7], and others [8]. Attitude observers in the special orthogonal group can be driven by reconstructed attitudes [9], which is the case of this paper. Filtering schemes based on the minimization of an "energy" function have also been developed more recently. These can be implemented using the Hamilton-Jacobi-Bellman theory [10], [11], but also by applying the variational mechanics formulation laid out in [12], such as the work in [13]. This work follows the latter approach.

Formations are groups of independent systems collaborating towards a given goal and operating within a limited space. In this paper, a heterogeneous formation is considered. Some of its applications are in the context of space missions, more specifically if the distance between the elements of the formation is large. Examples can be found, for instance, when synthesizing large aperture telescopes or long baseline interferometers far from Earth, or even when sampling spatially disperse phenomena such as the Earth's magnetotail [14]. Moreover, formations can potentially accomplish the same mission with relatively simpler systems, with increased reliability and redundancy. Space applications have high costs and risks, in general, and hence guidance systems of space formations have been studied since very early in the history of spaceflight [15]. Within formations, heterogeneous groups, which are defined by having non-identical individual elements [16], are of interest for their differentiation, even though their design and analysis may be more complex.

In the framework considered in this paper, attitude algebraic estimates are obtained from relative and inertial reference observations. These directions can be provided by vision sensors, such as large field of view position sensing diodes [17]. To measure inertial reference directions, different sensors can be used, such as magnetometers, sun sensors, or others, depending on the reference that is considered. The angular velocity is measured by rate gyros. All these sensors are used in spacecraft attitude estimation [18].

The main contribution of this work is the design of a locally exponentially stable attitude observer, which can be applied to the three-vehicle heterogeneous formation by using a deterministic reconstruction of the attitude and the angular velocity of each vehicle, based on the Lagrange-d'Alembert principle.

This paper is organized as follows. Section II describes the problem at hand and the attitude reconstruction algorithm. In Section III, the observer is derived based on variational mechanics. This method includes the construction of a Lagrangian that represents an energy-like function of the estimation errors and the application of the Lagrange-d'Alembert principle. The stability analysis follows and it is shown that the observer error converges to zero for almost all initial conditions and also that the origin is locally exponentially stable. Next, a first order discrete-time implementation

The work of P. Cruz was supported by the PhD Grant PD/BD/143143/2019 from FCT. This work was also supported by the Fundação para a Ciência e a Tecnologia (FCT) through LARSyS - FCT Project UIDB/50009/2020 and through the FCT project DECENTER [LISBOA-01-0145-FEDER-029605], funded by the Programa Operacional Regional de Lisboa 2020 and PIDDAC programs.

Pedro Cruz and Pedro Batista are with the Institute for Systems and Robotics, Laboratory for Robotics and Engineering Systems, at Instituto Superior Técnico, Universidade de Lisboa, Portugal.

Amit Sanyal is with the Department of Mechanical & Aerospace Engineering of the College of Engineering and Computer Science at Syracuse University, Syracuse, NY, United States.

[1]pfcruz@isr.tecnico.ulisboa.pt
[2]pbatista@isr.tecnico.ulisboa.pt
[3]aksanyal@syr.edu

of the filter is summarized in Section IV, which is derived from the discrete-time Lagrange-d'Alembert principle [19]. Finally, in Section V, the convergence characteristics and performance of the observer are assessed with numerical simulations.

## II. Problem statement

### A. Notation

Throughout this document, scalars are expressed in regular typeface and regular case, vectors are expressed in bold and regular case, and matrices are expressed in bold and upper case.

The symbol $\mathbf{0}$ represents the null vector or matrix and $\mathbf{I}$ represents the identity matrix. The dimensions of these parameters are given in subscript whenever they are necessary. The set of unit vectors in $\mathbb{R}^3$ is denoted by $\mathbb{S}^2 := \left\{\mathbf{x} \in \mathbb{R}^3 : \|\mathbf{x}\| = 1\right\}$. The special orthogonal group of dimension 3, which describes proper rotations, is denoted by $SO(3) := \left\{\mathbf{X} \in \mathbb{R}^{3\times 3} : \mathbf{X}\mathbf{X}^{\mathrm{T}} = \mathbf{X}^{\mathrm{T}}\mathbf{X} = \mathbf{I} \ \wedge \ \det(\mathbf{X}) = 1\right\}$. The skew-symmetric matrix parameterized by $\mathbf{x} \in \mathbb{R}^3$, which encodes the cross product operator in $\mathbb{R}^3$, is denoted by

$$\mathbf{S}(\mathbf{x}) := \begin{bmatrix} 0 & -x_3 & x_2 \\ x_3 & 0 & -x_1 \\ -x_2 & x_1 & 0 \end{bmatrix} ,$$

with $\mathbf{x} = [x_1\, x_2\, x_3]^{\mathrm{T}}$. Therefore, $\mathbf{S}(\mathbf{x})\,\mathbf{y} = \mathbf{x} \times \mathbf{y}$ and $\mathbf{S}^{-1}(.)$ denotes the unskew operator, i.e. $\mathbf{S}^{-1}(\mathbf{S}(\mathbf{x})) = \mathbf{x}$.

The rotation matrix in $SO(3)$ that transforms a given vector, in $\mathbb{R}^3$, expressed in the body-fixed frame of vehicle $j$ into the inertial frame, $j = 1, 2, 3$, is denoted by $\mathbf{R}_j^I$. If the rotation transforms a vector from the body-fixed frame of the $j$-th vehicle to the body-fixed frame of the $i$-th vehicle it is represented as $\mathbf{R}_j^i$, instead. The rotation matrix of an angle $\theta \in \mathbb{R}$ about the axis described by the unit vector $\mathbf{x} \in \mathbb{S}^2$ is denoted by $\mathbf{R}(\theta, \mathbf{x})$, which is written as [18]

$$\mathbf{R}(\theta, \mathbf{x}) := \cos(\theta)\,\mathbf{I} + (1 - \cos(\theta))\mathbf{x}\mathbf{x}^{\mathrm{T}} - \sin(\theta)\,\mathbf{S}(\mathbf{x}) \ . \quad (1)$$

Finally, the four-quadrant inverse tangent function is denoted by $\operatorname{atan2}(b, a)$, with $a, b \in \mathbb{R}$.

### B. Problem statement

Consider a three-vehicle formation, where each vehicle has a body-fixed coordinate frame. Each vehicle in the formation is equipped with vision-based sensors, which measure directions with respect to other vehicles in their lines of sight. Moreover, there are sensors that measure directions to inertial references, such as the direction to a cluster of stars, a magnetic field, or other references whose directions, in an inertial frame, are known *a priori*. Finally, it is assumed that three orthogonally-mounted rate gyros are available in each vehicle, which give a measurement of the angular velocity vector. These sensors give measurements in their respective body-fixed coordinate frames.

Each element of the formation measures its own angular velocity, one reference direction, and directions to at least one other vehicle. Vehicles 2 and 3, also called deputies, cannot measure the relative direction with respect to one another, because the line of sight between them is limited. Vehicle 1, also called chief, can measure the relative directions to the deputies. The formation and respective measurements are depicted in Fig. 1.

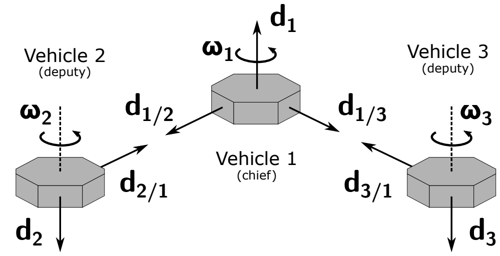


Fig. 1. Three-vehicle heterogeneous formation

The direction measurements are denoted by the letter $\mathbf{d}$. In the case of inertial reference measurements, the subscript indicates the vehicle taking the measurement, whereas in the case of relative direction measurements the subscript indicates both the vehicle taking the measurement and the respective target, i.e., the subscript $j/k$ indicates that the measurement was taken by vehicle j and it is a relative direction pointing to vehicle k. When representing the direction vectors in a coordinate frame, a left superscript indicates the frame where the measurement is represented, for instance, ${}^I\mathbf{d}_j$ denotes the inertial measurement taken by vehicle j represented in the inertial frame. The left superscript is omitted if the frame in which the vector is represented coincides with the body-fixed frame of the vehicle taking the measurement. Therefore, the four line of sight measurements are denoted as $\mathbf{d}_{1/2}$, $\mathbf{d}_{2/1}$, $\mathbf{d}_{1/3}$, and $\mathbf{d}_{3/1}$, the measurements of the inertial references are denoted as $\mathbf{d}_1$, $\mathbf{d}_2$, and $\mathbf{d}_3$, which, in the inertial frame, are respectively denoted as ${}^I\mathbf{d}_1$, ${}^I\mathbf{d}_2$, and ${}^I\mathbf{d}_3$ The value of the latter is known a priori, for example, the inertial directions to a set of stars. Finally, the angular velocity of each vehicle is respectively represented as $\boldsymbol{\omega}_1$, $\boldsymbol{\omega}_2$, and $\boldsymbol{\omega}_3$. The reference frame is indicated analogously to the direction vectors. Moreover, the angular velocities are assumed continuous, bounded, and unbiased. The attitude kinematics of the $j$-th vehicle is given by

$$\dot{\mathbf{R}}_j^I(t) = \mathbf{R}_j^I(t)\,\mathbf{S}(\boldsymbol{\omega}_j(t)) \ . \quad (2)$$

The observer internal representation of the attitude and the angular velocity is denoted with an hat. Furthermore, the observer kinematics is a copy of the true attitude kinematics, i.e.,

$$\dot{\hat{\mathbf{R}}}_j^I(t) = \hat{\mathbf{R}}_j^I(t)\,\mathbf{S}(\hat{\boldsymbol{\omega}}_j(t)) \ . \quad (3)$$

The problem addressed in this paper is the design of attitude estimators for $\left(\mathbf{R}_1^I, \mathbf{R}_2^I, \mathbf{R}_3^I\right)$ such that the error converges to zero for almost all initial conditions. The estimates of the relative attitudes $\left(\mathbf{R}_2^1, \mathbf{R}_3^1, \mathbf{R}_3^2\right)$ are derived from the inertial set, because these are defined by $\mathbf{R}_2^1 = \mathbf{R}_1^{I\,\mathrm{T}}\mathbf{R}_2^I$, $\mathbf{R}_3^1 = \mathbf{R}_1^{I\,\mathrm{T}}\mathbf{R}_3^I$, and $\mathbf{R}_3^2 = \mathbf{R}_2^{I\,\mathrm{T}}\mathbf{R}_3^I$, respectively.

### C. Attitude measurement

The direction vector measurements and the inertial references can be used to reconstruct both relative and inertial attitudes of the formation, by applying the deterministic algorithm in [20]. To summarize, such algorithm considers the axis and angle defined by

$$\mathbf{x}_1 := \begin{cases} \frac{\mathbf{d}_{2/1}-\mathbf{d}_{1/2}}{\left\|\mathbf{d}_{2/1}-\mathbf{d}_{1/2}\right\|} & \text{, if } \mathbf{d}_{2/1} \neq \mathbf{d}_{1/2} \\ \frac{\mathbf{S}(\mathbf{d}_1)\mathbf{d}_{1/2}}{\left\|\mathbf{S}(\mathbf{d}_1)\mathbf{d}_{1/2}\right\|} & \text{, if } \mathbf{d}_{2/1} = \mathbf{d}_{1/2} \end{cases},$$

and

$$\theta_2 := \operatorname{atan2}\left(a_{s_{12}}, a_{c_{12}}\right) \pm \arccos\left(\frac{a_{p_{12}}}{\sqrt{a_{s_{12}}^2 + a_{c_{12}}^2}}\right), \quad (4)$$

where $a_{s_{12}}$, $a_{c_{12}}$, and $a_{p_{12}}$ are scalar coefficients which depend on the measurements. Then, the relative attitude candidate is given as $\left(\mathbf{R}_2^1\right)_X = \mathbf{R}\left(\theta_2, -\mathbf{d}_{1/2}\right)\mathbf{R}\left(\pi, \mathbf{x}_1\right)$ . Therefore, the respective inertial candidate $\left(\mathbf{R}_1^I\right)_X$ results from the TRIAD algorithm with the measurement pairs $\left({}^I\mathbf{d}_1, \mathbf{d}_1\right)$ and $\left({}^I\mathbf{d}_2, \left(\mathbf{R}_2^1\right)_X \mathbf{d}_2\right)$. The different candidates result from the different signs in (4).

The analogous relative candidate $\left(\mathbf{R}_3^1\right)_Y$ is obtained considering $\left(\mathbf{R}_3^1\right)_Y = \mathbf{R}\left(\theta_4, -\mathbf{d}_{1/3}\right)\mathbf{R}\left(\pi, \mathbf{x}_3\right)$ with analogous $\mathbf{x}_3$ and $\theta_4$. The respective inertial candidate $\left(\mathbf{R}_1^I\right)_Y$ results from the TRIAD algorithm with $\left({}^I\mathbf{d}_1, \mathbf{d}_1\right)$ and $\left({}^I\mathbf{d}_3, \left(\mathbf{R}_3^1\right)_Y \mathbf{d}_3\right)$.

After comparing the four candidates for $\mathbf{R}_1^I$, the algorithm selects the correct attitude candidate by checking the candidate's compatibility. Once the solutions for $\mathbf{R}_1^I$, $\mathbf{R}_2^1$, and $\mathbf{R}_3^1$ are available, the solutions for $\mathbf{R}_2^I$ and $\mathbf{R}_3^I$ follow immediately from $\mathbf{R}_2^I = \mathbf{R}_1^I\mathbf{R}_2^1$ and $\mathbf{R}_3^I = \mathbf{R}_1^I\mathbf{R}_3^1$.

In general, there is a unique solution. Nonetheless, in specific configurations, there may be multiple solutions. Thus, it is assumed that the configuration is such that the deterministic algorithm gives a unique solution, see [21] for the characterization of the conditions of the solution. The observer design proposed in the sequel uses this attitude reconstruction.

## III. Observer Design

The ensuing attitude observer assumes that the reconstruction of the inertial attitude of each vehicle from the measurement set is available, taking advantage of the algorithm described in the previous section. Therefore, a single vehicle is considered throughout this section, because the same observer can be employed individually by each vehicle. The observer is a direct result of the application of the Lagrange-d'Alembert principle of variational mechanics. The method relies on a Lagrangian function, which is constructed to represent an energy-like function of the estimation errors. Then, after computing the first variation of the action functional and adding a dissipation term, the Lagrange-d'Alembert principle gives the dynamics of the observer feedback term. For readability, the time dependence of the variables is omitted in this section.

### A. Lagrangian

The observer internal representation of the angular velocity, for vehicle $j$, is given by the difference between the true angular velocity and a feedback term, $\boldsymbol{\phi}_j$, as follows

$$\hat{\boldsymbol{\omega}}_j = \boldsymbol{\omega}_j - \boldsymbol{\phi}_j . \quad (5)$$

Then, consider the kinetic energy-like function

$$T_j := \frac{m_j}{2}\left(\boldsymbol{\omega}_j - \hat{\boldsymbol{\omega}}_j\right)^{\mathrm{T}}\left(\boldsymbol{\omega}_j - \hat{\boldsymbol{\omega}}_j\right) ,$$

where $m_j$ is a positive weight constant. The inertial attitude error matrix of vehicle $j$ is given by

$$\mathbf{Q}_j^I = \mathbf{R}_j^I\hat{\mathbf{R}}_j^{I\mathrm{T}}. \quad (6)$$

Then, consider the potential energy-like function

$$U_j := p_j \operatorname{trace}\left(\mathbf{I} - \mathbf{Q}_j^I\right) ,$$

where $p_j$ is a positive weight constant. Finally, the Lagrangian of the formation is given by $\mathcal{L}_j = T_j - U_j$.

### B. First variation of the action functional

The action functional is defined as the time integral of the Lagrangian function. Thus, its first variation is given by

$$\delta s_j = \int_{t_0}^{t_f} \delta\mathcal{L}_j \, dt = \int_{t_0}^{t_f} \delta T_j - \delta U_j \, dt , \quad (7)$$

where $t_0$ and $t_f$ are the initial and final time of estimation, respectively. The estimated inertial attitude first variation of the $j$-th vehicle is given as $\delta\hat{\mathbf{R}}_j^I = \hat{\mathbf{R}}_j^I\mathbf{S}\left(\eta_j\right)$, where $\eta_j$ is a perturbation function. Moreover, from the attitude kinematics, the first variation of the observer internal angular velocity is given by $\delta\hat{\boldsymbol{\omega}}_j = \dot{\eta}_j + \mathbf{S}\left(\hat{\boldsymbol{\omega}}_j\right)\eta_j$ [12]. Therefore, the first variation of the kinematic term is expressed as

$$\delta T_j = -m_j\boldsymbol{\phi}_j^{\mathrm{T}}\left(\dot{\eta}_j + \mathbf{S}\left(\hat{\boldsymbol{\omega}}_j\right)\eta_j\right) . \quad (8)$$

The first variation of the potential term is given by

$$\delta U_j = p_j \operatorname{trace}\left(\hat{\mathbf{R}}_j^{I\mathrm{T}}\mathbf{R}_j^I\mathbf{S}\left(\eta_j\right)\right) ,$$

which, expressing $\hat{\mathbf{R}}_j^{I\mathrm{T}}\mathbf{R}_j^I$ as the sum of a symmetric and skew symmetric matrix, then recalling that the trace of the product between a symmetric and skew symmetric matrix is zero, gives $\delta U_j = p_j \operatorname{trace}\left(\frac{1}{2}\left(\hat{\mathbf{R}}_j^{I\mathrm{T}}\mathbf{R}_j^I - \mathbf{R}_j^{I\mathrm{T}}\hat{\mathbf{R}}_j^I\right)\mathbf{S}\left(\eta_j\right)\right)$. Lastly, from $\operatorname{trace}\left(\mathbf{S}\left(\mathbf{a}\right)\mathbf{S}\left(\mathbf{b}\right)\right) = -2\mathbf{a}^{\mathrm{T}}\mathbf{b}$ with $\mathbf{a}, \mathbf{b} \in \mathbb{R}^3$, it follows that

$$\delta U_j = -p_j\mathbf{S}^{-1}\left(\hat{\mathbf{R}}_j^{I\mathrm{T}}\mathbf{R}_j^I - \mathbf{R}_j^{I\mathrm{T}}\hat{\mathbf{R}}_j^I\right)^{\mathrm{T}}\eta_j . \quad (9)$$

### C. Observer feedback dynamics

Consider a dissipation term given by $\left(\mathbf{D}_j\boldsymbol{\phi}_j\right)^{\mathrm{T}}\eta_j$, with $\mathbf{D}_j$ positive definite. Then, applying the Lagrange-d'Alembert principle to the sum of the action functional and dissipation terms, and recalling (7), (8), and (9), yields

$$\int_{t_0}^{t_f} -m_j\boldsymbol{\phi}_j^{\mathrm{T}}\dot{\eta}_j - m_j\boldsymbol{\phi}_j^{\mathrm{T}}\mathbf{S}\left(\hat{\boldsymbol{\omega}}_j\right)\eta_j + p_j\mathbf{S}^{-1}\left(\mathbf{M}_j\right)^{\mathrm{T}}\eta_j + \left(\mathbf{D}_j\boldsymbol{\phi}_j\right)^{\mathrm{T}}\eta_j \, dt = 0 ,$$

where $\mathbf{M}_j := \hat{\mathbf{R}}_j^{I\mathrm{T}} \mathbf{R}_j^I - \mathbf{R}_j^{I\mathrm{T}} \hat{\mathbf{R}}_j^I$. Since the perturbation function is zero at $t_0$ and at $t_f$, then integrating the first term by parts gives

$$\int_{t_0}^{t_f} \left[ m_j \dot{\boldsymbol{\phi}}_j + \left( m_j \mathbf{S}\left(\hat{\boldsymbol{\omega}}_j\right) + \mathbf{D}_j \right) \boldsymbol{\phi}_j + p_j \mathbf{S}^{-1}(\mathbf{M}_j) \right]^{\mathrm{T}} \eta_j dt = 0.$$

Finally, the fundamental lemma of the calculus of variations results in an equation that encodes the estimator feedback term dynamics. Thus, the observer equations are given by

$$\dot{\hat{\mathbf{R}}}_j^I = \hat{\mathbf{R}}_j^I \mathbf{S}\left(\hat{\boldsymbol{\omega}}_j\right)$$

and

$$m_j \dot{\boldsymbol{\phi}}_j = -\left( m_j \mathbf{S}\left(\hat{\boldsymbol{\omega}}_j\right) + \mathbf{D}_j \right) \boldsymbol{\phi}_j - p_j \mathbf{S}^{-1}(\mathbf{M}_j) \ .$$

### D. Observer stability

In this section, the error dynamics are studied under the assumption that the measurements are free of noise. In such conditions, it is shown that the error converges asymptotically to zero for almost all initial configurations and that the origin is locally exponentially stable. The attitude observer performance in the presence of sensor noise is assessed later on.

The error system dynamics, considering the $j$-th vehicle, are given by

$$\dot{\mathbf{Q}}_j^I = \mathbf{S}\left(\mathbf{R}_j^I \boldsymbol{\phi}_j\right) \mathbf{Q}_j^I \tag{10a}$$

and

$$\begin{aligned} m_j \dot{\boldsymbol{\phi}}_j = &- p_j \mathbf{S}^{-1}\!\left(\mathbf{R}_j^{I\mathrm{T}} \left[\mathbf{Q}_j^{IT} - \mathbf{Q}_j^I\right] \mathbf{R}_j^I\right) \\ &- \left[ m_j \mathbf{S}\left(\hat{\boldsymbol{\omega}}_j\right) + \mathbf{D}_j^I \right] \boldsymbol{\phi}_j \end{aligned} \ . \tag{10b}$$

*1) Equilibrium Points:* Understanding the equilibrium properties of the error system is fundamental to characterize its stability. To find the equilibrium points of (10), substitute $\dot{\mathbf{Q}}_j^I = \mathbf{0}$ and $\dot{\boldsymbol{\phi}}_j = \mathbf{0}$, which implies that $\boldsymbol{\phi}_j = \mathbf{0}$ and

$$\mathbf{Q}_j^I = \mathbf{Q}_j^{IT} \ . \tag{11}$$

Therefore, all symmetric error matrices are equilibrium points of the error system dynamics, when $\boldsymbol{\phi}_j = 0$. Next, express $\mathbf{Q}_j^I$ using the Euler axis/angle parameterization, with axis and angle respectively given by $\mathbf{e} \in \mathbb{S}^2$ and $\epsilon \in \mathbb{R}$, and rewrite (11) as $\mathbf{Q}_j^I \mathbf{Q}_j^I = \mathbf{R}\left(2\epsilon, \mathbf{e}\right) = \mathbf{I}$. From (1) and the appropriate trigonometric relations, it follows that

$$\sin\left(\epsilon\right) \left[ \sin\left(\epsilon\right) \left( \mathbf{e}\mathbf{e}^{\mathrm{T}} - \mathbf{I} \right) - \cos\left(\epsilon\right) \mathbf{S}\left(\mathbf{e}\right) \right] = \mathbf{0} \, . \tag{12}$$

If $\sin\left(\epsilon\right) = 0$, then $\epsilon = k\pi$, $k \in \mathbb{Z}$. Otherwise, if $\sin\left(\epsilon\right) \neq 0$, then $\sin\left(\epsilon\right) \left( \mathbf{e}\mathbf{e}^{\mathrm{T}} - \mathbf{I} \right) = \cos\left(\epsilon\right) \mathbf{S}\left(\mathbf{e}\right)$, which can only be satisfied if all elements of $\mathbf{e}$ are $1$ or $-1$. Since $\mathbf{e}$ is assumed to have unit length, then such $\mathbf{e}$ would violate the assumptions. Therefore, the solution for (12) is $\epsilon = k\pi$, $k \in \mathbb{Z}$.

For a more compact representation of the equilibrium points, recall that $\mathrm{trace}\left(\mathbf{Q}_j^I\right) = 1 + 2\cos\left(\epsilon\right)$. Hence, for $\epsilon = 0 + 2k\pi$, $\mathrm{trace}\left(\mathbf{Q}_j^I\right) = 3$ and for $\epsilon = \pi + 2k\pi$, $\mathrm{trace}\left(\mathbf{Q}_j^I\right) = -1$. Then, define

$$S_j := \left\{ \left(\mathbf{Q}_j^I, \boldsymbol{\phi}_j\right) \middle| \mathrm{trace}\left(\mathbf{Q}_j^I\right) = 3,\ \boldsymbol{\phi}_j = \mathbf{0} \right\}, \tag{13}$$

which is the desired equilibrium point (zero estimation error). Define also the undesired equilibrium set as

$$U_j := \left\{ \left(\mathbf{Q}_j^I, \boldsymbol{\phi}_j\right) \middle| \mathrm{trace}\left(\mathbf{Q}_j^I\right) = -1,\ \boldsymbol{\phi}_j = \mathbf{0} \right\}. \tag{14}$$

The set of all equilibrium points is the union of both sets, which is denoted as $E_j = S_j \cup U_j$.

*2) Observer stability:* The stability characteristics of the observer are detailed in the following theorem.

*Theorem 1:* Consider the error system (10) and the equilibrium sets $S_j$ and $U_j$, defined in (13) and (14), respectively. Assume that $\boldsymbol{\omega}_j$, $j = 1, 2, 3$ is bounded. Then:

1) the set $U_j$ is forward invariant and unstable relative to the error dynamics (10);
2) the set $S_j$ is locally exponentially stable; and
3) the error converges to $S_j$ for almost all initial conditions $\notin U_j$.

*Proof:* The first part of the theorem can be shown with the Lyapunov function given by

$$V\left(t\right) = \sum_{j=1}^{3} \frac{m_j}{2} \boldsymbol{\phi}_j^{\mathrm{T}} \boldsymbol{\phi}_j + p_j \mathrm{trace}\left(\mathbf{I} - \mathbf{Q}_j^I\right) \ .$$

Computing $\dot{V}\left(t\right)$ leads to the conclusion that $\boldsymbol{\phi}_j$ is bounded by the initial conditions. Applying Barbalat's lemma it follows that $\boldsymbol{\phi}_j\left(t\right)$ converges to zero. Thus, $E_j = S_j \cup U_j$ is the largest forward invariant set. Then, the linearization of the error system (10) about a general point of $U_j$, considering $\mathbf{Q}_j^I \approx \mathbf{S}\left(\mathbf{x}\right) + \mathbf{R}\left(\pi, \mathbf{e}\right)$ and $\boldsymbol{\phi}_j \approx \mathbf{y}$, yields an unstable system with both positive and negative eigenvalues.

The second part of the lemma is shown through the linearization about the origin, i.e., $S_j$, considering $\mathbf{Q}_j^I \approx \mathbf{S}\left(\mathbf{x}\right) + \mathbf{I}$ and $\boldsymbol{\phi}_j \approx \mathbf{y}$. The result is an exponentially stable linear system, and thus (10) is locally asymptotically stable at the origin.

Finally, since the linearization of the unstable set has both positive and negative eigenvalues, then there will be trajectories that converge to $U_j$ along the center stable manifold [22]. From classical center manifold theory, those trajectories are zero-measure. Since $U_j$ is a zero-measure subset of $SO(3) \times \mathbb{R}^3$, the proof is concluded. ∎

## IV. Discrete-time observer

The implementation of the observer from the previous section requires its discrete-time version, which is a Lie group variational integrator (LGVI). The measurements are assumed to be obtained at an appropriate constant rate in discrete-time. The stability properties are the same for both versions of the observer since LGVI maintain the properties of variational mechanics [12].

The derivation of the discrete-time version relies on the discretization of the action functional and attitude kinematics, which combined with the discrete-time formulation of the Lagrange-d'Alembert principle result in

$$\dot{\hat{\mathbf{R}}}_{j_{k+1}}^I = \hat{\mathbf{R}}_{j_k}^I \exp\left[\Delta t \mathbf{S}\left(\hat{\boldsymbol{\omega}}_{j_k}\right)\right] \tag{15a}$$

and

$$m_j\dot{\boldsymbol{\phi}}_{j_{k+1}} = \exp\left[-\Delta t\mathbf{S}\left(\hat{\boldsymbol{\omega}}_{j_k}\right)\right]\Big[m_j\boldsymbol{\phi}_{j_k} \\ -\Delta t\mathbf{D}_j\boldsymbol{\phi}_{j_k} - \Delta t p_j \mathbf{S}^{-1}\!\left(\mathbf{M}_{j_{k+1}}\right)\Big] \ , \quad (15b)$$

with $j = 1, 2, 3$, $\mathbf{M}_{j_{k+1}} = \hat{\mathbf{R}}^{I\,T}_{j_{k+1}}\mathbf{R}^{I}_{j_{k+1}} - \mathbf{R}^{I\,T}_{j_{k+1}}\hat{\mathbf{R}}^{I}_{j_{k+1}}$, and $\hat{\boldsymbol{\omega}}_{j_k} = \boldsymbol{\omega}_{j_k} - \boldsymbol{\phi}_{j_k}$. For further details about the derivation of these equations, see [12].

## V. SIMULATION

To assess the performance of the proposed solution in the presence of sensor noise, numerical simulations are presented in this section. The simulations consider a three vehicle formation configuration, as described in the problem statement section.

### A. Measurement Model

Line of sight and inertial reference measurements follow the model of the large field of view position sensing diode [17]. In this model, the sensor gives two coordinates, $\mathbf{m} = [\chi, \psi]$, whose measurement is expressed as

$$\mathbf{m_m} = \mathbf{m} + \mathbf{n} \ ,$$

i.e. the sum of the true value with a zero mean random Gaussian noise, $\mathbf{n} \sim \mathcal{N}\left(\mathbf{0}, \mathbf{P}^F\right)$. The covariance in the focal plane is given by

$$\mathbf{P}^F = \frac{\sigma_d^2}{1 + (\chi^2 + \psi^2)} \begin{bmatrix} \left(1+\chi^2\right)^2 & (\chi\psi)^2 \\ (\chi\psi)^2 & \left(1+\psi^2\right)^2 \end{bmatrix} \ ,$$

where $\sigma_d$ is the standard deviation of the focal coordinates. The transformation from the focal coordinates into the unit vector is given by

$${}^{s}\mathbf{d} = \frac{1}{\sqrt{1+\chi^2+\psi^2}}\left[\chi, \psi, 1\right]^{\mathrm{T}} \ ,$$

where the focal length is assumed to be equal to one. The angular velocity measurement follows the discrete-time unbiased rate gyro model given by [18]

$$\boldsymbol{\omega}_{j_m} = \boldsymbol{\omega}_j + \left(\frac{\sigma^2_{\boldsymbol{\omega}_\mathrm{j}}}{\Delta t}\right)^{\frac{1}{2}} \mathbf{N}_j \ ,$$

where $\boldsymbol{\omega}_{j_m}$ is the angular velocity measurement, $\sigma_{\boldsymbol{\omega}_\mathrm{j}}$ is the standard deviation of the noise, and $\mathbf{N}_j \sim \mathcal{N}\left(\mathbf{0}, \mathbf{I}\right)$.

### B. Motion Model

The true values of the attitude follow the kinematics (2). Moreover, the model of the dynamics for a rigid body, which can represent spacecraft in flight, determines the ground truth of the angular velocity for each vehicle. Considering vehicle $j$, such model is given by

$$\dot{\boldsymbol{\omega}}_j = \mathbf{J}_j^{-1}\left(\boldsymbol{\tau}_{F_j} - \mathbf{S}\left(\boldsymbol{\omega}_j\right)\mathbf{J}_j\boldsymbol{\omega}_j\right) \ , \qquad (16)$$

where $\boldsymbol{\tau}_{F_j}$ represents an external moment applied to each vehicle given in $\mathrm{N\,m^{-1}}$, and $\mathbf{J}_j$ denotes the moment of inertia given in $\mathrm{kg\,m^2}$.

### C. Initial conditions

In this simulation, the initial attitudes are given by

$$\mathbf{R}_1^I = \begin{bmatrix} 0 & 1 & 0 \\ -1 & 0 & 0 \\ 0 & 0 & 1 \end{bmatrix}, \mathbf{R}_2^I = \begin{bmatrix} 1 & 0 & 0 \\ 0 & 0 & 1 \\ 0 & -1 & 0 \end{bmatrix}, \mathbf{R}_3^I = \begin{bmatrix} 1 & 0 & 0 \\ 0 & 1 & 0 \\ 0 & 0 & 1 \end{bmatrix} \ ,$$

the inertial references are given by ${}^{I}\mathbf{d}_1 = [1\,0\,0]^{\mathrm{T}}$, ${}^{I}\mathbf{d}_2 = \left[0\ \frac{1}{\sqrt{2}}\ \frac{1}{\sqrt{2}}\right]^{\mathrm{T}}$, ${}^{I}\mathbf{d}_3 = \left[\frac{1}{\sqrt{3}}\ \frac{1}{\sqrt{3}}\ \frac{1}{\sqrt{3}}\right]^{\mathrm{T}}$, and the initial line of sight relative directions are given by ${}^{I}\mathbf{d}_{1/2} = \mathbf{R}_1^I\mathbf{d}_{1/2} = \left[\frac{2}{\sqrt{5}}\ \frac{1}{\sqrt{5}}\ 0\right]^{\mathrm{T}}$ and ${}^{I}\mathbf{d}_{1/3} = \mathbf{R}_1^I\mathbf{d}_{1/3} = \left[\frac{1}{\sqrt{5}}\ 0\ \frac{2}{\sqrt{5}}\right]^{\mathrm{T}}$. Finally, the initial angular velocities are given by $\boldsymbol{\omega}_1 = \boldsymbol{\omega}_2 = \boldsymbol{\omega}_3 = [0.1\ 0.2\ 0.3]^{\mathrm{T}}$, in radians per second.

### D. Setup

The configuration choice ensures that the vision-based measurements are far from ambiguous cases [20], [21]. Furthermore, the external torque applied to each vehicle is a sinusoidal signal given as $\boldsymbol{\tau}_{F_j} = 0.1\sin\left(f\Delta t + 0.1j\right)$, with $j=1$,2,3, and $f=1\ \mathrm{rad\,s^{-1}}$. Thus, all assumptions are satisfied.

The vehicles are assumed identical and cylindrical, with mass, height, and radius given, respectively, by $m = 120$ kg, $r = 1$m, and $h = 2$m. Therefore, the moments of inertia are given by a diagonal matrix with the entries respectively given by $\frac{m}{12}\left(3r^2 + h^2\right)$, $\frac{m}{12}\left(3r^2 + h^2\right)$, and $\frac{m}{2}r^2$.

For simplicity, the vision-based sensors are assumed to have a sensor plane facing each of the body-fixed frame axes. Then, the measurement is taken in the plane orthogonal to the highest component of the vector. This strategy ensures that the measurement set is always complete. Moreover, the vision-based true values are constant in the inertial frame, in order to easily avoid the ambiguous configurations. The standard deviation of the measurements in the focal frame is $\sigma_d = 17\times10^{-6}$ rad, whereas the standard deviation of the rate gyros is $\sigma_{\boldsymbol{\omega}_j} = 4\times10^{-5}$.

The observer initial estimates are assumed to be at the origin, $\left(\hat{\mathbf{R}}_j^I(t_0), \hat{\boldsymbol{\omega}}_j(t_0)\right) = (\mathbf{I}, \mathbf{0})$, for all vehicles. Moreover, the weight constants are set to 1 and the dissipation matrices are set to the identity, i.e $m_j = p_j = 1$ and $\mathbf{D}_j = \mathbf{I}$.

The simulation interval is 50 seconds with a time step of 0.01 seconds. In each iteration, the true values are updated according to (2) and (16). Then, the vision sensor and rate gyro measurements are generated following the noise models described before. Next, from the vision-based measurements, the deterministic algorithm gives a measurement for each attitude. Finally, the attitude estimates are computed with (15), first the new attitude estimate and then the new feedback term, by solving the respective equation numerically. The errors result from the comparison between the estimated attitude and the true values.

### E. Results

The errors are given by the norm of the 3-2-1 sequence of Euler angles [18], which are computed from the error matrix (6). Therefore, Figs.2, 3, and 4 show the error magnitude for the inertial attitudes of the formation, which converge to an error close to the noise standard deviation magnitude of the sensors.

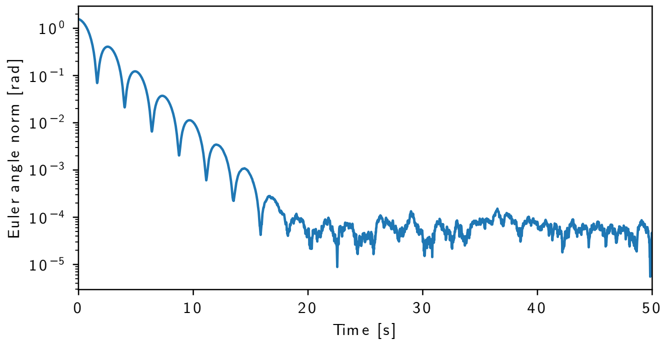


Fig. 2. Results for $\mathbf{Q}_1^I$

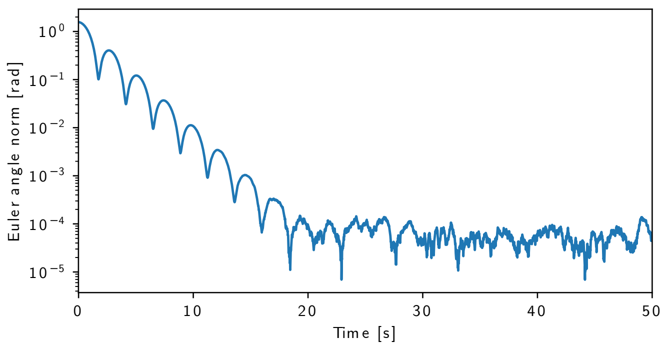


Fig. 3. Results for $\mathbf{Q}_2^I$

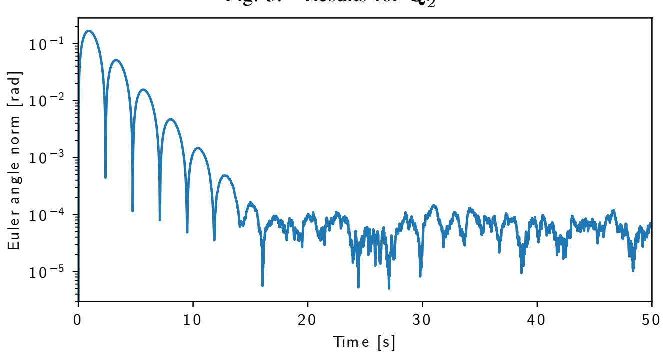


Fig. 4. Results for $\mathbf{Q}_3^I$

## VI. Conclusions

An attitude observer was designed based on the Lagrange-d'Alembert principle of variational mechanics, with application to the three-vehicle heterogeneous formations. The observer error is locally exponentially stable and converges to the origin for almost all initial conditions. The remaining equilibrium points are unstable and a zero measure subset of the domain. Numerical simulations were implemented to assess performance of the solution with sensor noise.

## References

[1] H. Black, "A passive system for determining the attitude of a satellite," *AIAA Journal*, vol. 2, no. 7, pp. 1350–1351, jul 1964.

[2] G. Wahba, "A least squares estimate of satellite attitude," *SIAM Review*, vol. 7, no. 3, p. 409, 1965.

[3] J. L. Farrell, J. C. Stuelpnagel, R. H. Wessner, J. R. Velman, and J. E. Brook, "A least squares estimate of satellite attitude (grace wahba)," *SIAM Review*, vol. 8, no. 3, pp. 384–386, 1966.

[4] F. L. Markley, "Attitude determination using vector observations: A fast optimal matrix," *Journal of the Astronautical Sciences*, vol. 41, no. 2, pp. 261–280, 1993.

[5] J. Farrell, "Attitude determination by kalman filtering," *Automatica*, vol. 6, no. 3, pp. 419 – 430, 1970.

[6] A. K. Sanyal, T. Lee, M. Leok, and N. H. McClamroch, "Global optimal attitude estimation using uncertainty ellipsoids," *Systems & Control Letters*, vol. 57, no. 3, pp. 236 – 245, 2008.

[7] P. Batista, C. Silvestre, and P. Oliveira, "Globally exponentially stable cascade observers for attitude estimation," *Control Engineering Practice*, vol. 20, no. 2, pp. 148 – 155, 2012.

[8] J. L. Crassidis, F. L. Markley, and Y. Cheng, "Survey of nonlinear attitude estimation methods," *Journal of Guidance, Control, and Dynamics*, vol. 30, no. 1, pp. 12–28, 2007.

[9] R. Mahony, T. Hamel, and J. Pflimlin, "Nonlinear complementary filters on the special orthogonal group," *IEEE Transactions on Automatic Control*, vol. 53, no. 5, pp. 1203–1218, 2008.

[10] A. P. Aguiar and J. P. Hespanha, "Minimum-energy state estimation for systems with perspective outputs," *IEEE Transactions on Automatic Control*, vol. 51, no. 2, pp. 226–241, Feb 2006.

[11] M. Zamani, J. Trumpf, and R. Mahony, "Near-optimal deterministic filtering on the rotation group," *IEEE Transactions on Automatic Control*, vol. 56, no. 6, pp. 1411–1414, June 2011.

[12] M. Izadi and A. K. Sanyal, "Rigid body attitude estimation based on the lagrange–d'alembert principle," *Automatica*, vol. 50, no. 10, pp. 2570 – 2577, 2014.

[13] G. Misra, M. Izadi, A. Sanyal, and D. Scheeres, "Coupled orbit–attitude dynamics and relative state estimation of spacecraft near small Solar System bodies," *Advances in Space Research*, vol. 57, no. 8, pp. 1747–1761, Apr. 2016.

[14] R. Cesarone, D. Abraham, and L. Deutsch, "Prospects for a next-generation deep-space network," *Proceedings of the IEEE*, vol. 95, pp. 1902 – 1915, 11 2007.

[15] D. P. Scharf, F. Y. Hadaegh, and S. R. Ploen, "A survey of spacecraft formation flying guidance and control (part 1): guidance," in *Proceedings of the 2003 American Control Conference, 2003.*, vol. 2, June 2003, pp. 1733–1739.

[16] Y. Cao, A. Fukunaga, and A. Kahng, "Cooperative mobile robotics: Antecedents and directions," *Autonomous Robots*, vol. 4, pp. 7–27, 1997.

[17] Y. Cheng, J. L. Crassidis, and F. L. Markley, "Attitude estimation for large field-of-view sensors," *Journal of the Astronautical Sciences*, vol. 54, no. 3, pp. 433–448, dec 2006.

[18] F. L. Markley and J. L. Crassidis, *Fundamentals of Spacecraft Attitude Determination and Control*, 1st ed. New York: Microcosm Press and Springer, 2014.

[19] J. E. Marsden and M. West, "Discrete mechanics and variational integrators," *Acta Numerica*, vol. 10, p. 357–514, 2001.

[20] P. Cruz and P. Batista, "A solution for the attitude determination of three-vehicle heterogeneous formations," *Aerospace Science and Technology*, vol. 93, p. 105275, 2019.

[21] ——, "Special cases in the attitude determination of three-vehicle heterogeneous formations," in *2020 7th International Conference on Control, Decision and Information Technologies (CoDIT)*, vol. 1, 2020, pp. 136–141.

[22] H. Khalil, *Nonlinear Systems*, 3rd ed., ser. Pearson Education. Prentice Hall, 2002.